Novel targets in the liver to treat cardiometabolic diseases

Ge, X.

CHAPTER 3

DHCR24 inhibitor SH42 increases desmosterol without preventing atherosclerosis development in mice

Xiaoke Ge, Bram Slütter, Joost M. Lambooij, Enchen Zhou, Zhixiong Ying, Ceren Agirman, Marieke Heijink, Antoine Rimbert, Bruno Guigas, Johan Kuiper, Christoph Müller, Franz Bracher, Martin Giera, Sander Kooijman, Patrick C.N. Rensen, Yanan Wang, Milena Schönke

iScience 2024, 27: 109830

Abstract

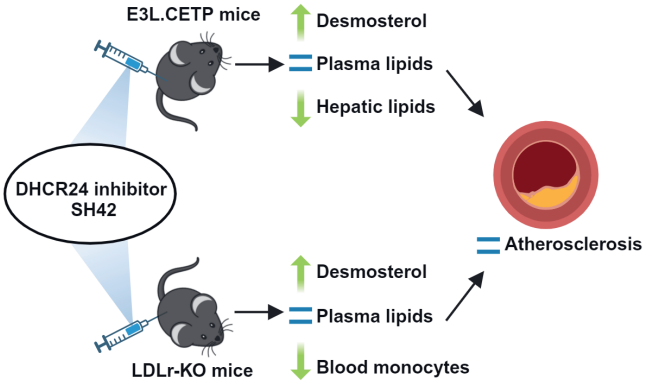

The liver X receptor (LXR) is considered a therapeutic target for atherosclerosis treatment, but synthetic LXR agonists generally also cause hepatic steatosis and hypertriglyceridemia. Desmosterol, a final intermediate in cholesterol biosynthesis, has been identified as a selective LXR ligand that suppresses inflammation without inducing lipogenesis. Δ24-Dehydrocholesterol reductase (DHCR24) converts desmosterol into cholesterol, and we previously showed that the DHCR24 inhibitor SH42 increases desmosterol to activate LXR and attenuate experimental peritonitis and metabolic dysfunction-associated steatotic liver disease. Here, we aimed to evaluate the effect of SH42 on atherosclerosis development in APOE*3-Leiden.CETP mice and LDL receptor knockout mice, models for lipid- and inflammation-driven atherosclerosis, respectively. In both models, SH42 increased desmosterol without affecting plasma lipids. While reducing liver lipids in APOE*3-Leiden.CETP mice, and regulating populations of circulating monocytes in LDL receptor knockout mice, SH42 did not attenuate atherosclerosis in either model.

Introduction

Cardiovascular diseases (CVDs) are the leading cause of mortality worldwide, responsible for an estimated 32% of all global deaths.[1] The main underlying cause of CVDs is atherosclerosis, which is characterized by the buildup of lipids and immune cells inside the walls of arteries. Hypercholesterolemia drives the accumulation of low-density lipoproteins (LDL) in artery walls. LDL is taken up by monocyte-derived macrophages that turn into foam cells, resulting in fatty streaks in the intima of vessels. Foam cell generation induces the production and secretion of pro-inflammatory cytokines that further stimulate monocyte recruitment and transdifferentiation of smooth muscle cells into macrophage-like cells, supporting a chronic inflammatory response and eventually acceleration of atherosclerotic lesion development.[2]

Numerous studies have demonstrated that activating liver X receptors (LXR), crucial regulators of lipid metabolism and immune responses, protects against atherosclerosis development in animals.[3-5] LXR activation in macrophages promotes reverse cholesterol transport, i.e. increases the efflux of cholesterol from macrophages towards the liver, through upregulation of the expression of macrophage genes involved in cholesterol efflux including ATP-binding cassette transporter A1 (ABCA1) and ATP-binding cassette transporter G1 (ABCG1). Accordingly, foam cell formation is reduced and inflammatory responses are suppressed.[4,6] However, LXR activation by synthetic LXR agonists such as T0901317 and GW3965 also stimulates lipogenesis in hepatocytes *via* the activation of sterol regulatory element-binding transcription proteins (SREBP), which causes hepatic steatosis and hypertriglyceridemia.[7-11] Accordingly, clinical trials using synthetic LXR agonists showed dyslipidemic side effects,[12] based on which clinical programs with LXR agonists were discontinued.

Desmosterol, the last intermediate in the Bloch pathway of *de novo* cholesterol synthesis, is involved in selective reprogramming of lipid metabolism and suppression of inflammation by activating LXR target genes and inhibiting SREBP activity by binding to SREBP cleavage-activating protein in macrophages.[13] On the contrary, desmosterol does not seem to activate LXR in hepatocytes.[14] This implies that increasing desmosterol concentrations may be a potential safe strategy in the treatment of diseases driven by hypercholesterolemia and inflammation. We have previously generated SH42 as inhibitor of Δ24-dehydrocholesterol reductase (DHCR24), the enzyme catalyzing conversion of desmosterol into cholesterol,[15] and showed that SH42 treatment increases desmosterol levels to enhance inflammation resolution in a peritonitis mouse model.[16] Recently, we also demonstrated that SH42 effectively inhibits liver inflammation by reducing Kupffer cell activation and monocyte infiltration, hence preventing diet-induced hepatic inflammation and steatosis.[17] Importantly, LXR activation through desmosterol accumulation did not result in

hypertriglyceridemia in our studies. The present study aimed to investigate whether SH42 could also effectively reduce atherosclerosis development. To this end, we used APOE*3-Leiden.CETP (E3L.CETP) mice, a well-established human-like model for lipid-driven atherosclerosis, and LDL receptor knockout (LDLr-KO) mice, a model for inflammation-driven atherosclerosis.[18]

Method details

Experimental Model and Study Participant Details Animals and treatments

In experiments 1 and 2, female E3L.CETP mice (8–12 weeks of age) were used. These mice were generated by crossbreeding hemizygous APOE*3-Leiden (E3L) mice with mice expressing human cholesteryl ester transfer protein (CETP), both on a C57BL/6J background, as described previously.[19] The mice were fed a Western-type diet (Ssniff Spezialdiäten GmbH, Germany) containing 16% fat and 0.15% cholesterol. Following a 3-week dietary run-in period to induce hyperlipidemia, mice were block randomized using RandoMice v1.1.6[20] into two groups balanced for plasma lipid levels and body composition and treated either with the DHCR24 inhibitor SH42 (0.5 mg dissolved in 7.5 µL ethanol and 7.5 µL Cremophor EL in 135 µL saline) or vehicle 3 times per week for 6 weeks in experiment 1 (n=11-12 per group) and for 15 weeks in experiment 2 (n=16 per group) *via* intraperitoneal injection.

In experiment 3, male LDLr-KO mice (8–12 weeks of age) on a C57BL/6J background were used (B6.129S7-Ldlrtm1Her/J; Jackson Laboratory, USA). After block-randomization into two groups (n=13-15 per group) as described above, the mice were fed a Western-type diet (Ssniff Spezialdiäten GmbH, Germany) containing 16% fat and 0.25% cholesterol, and treated with either 0.5 mg DHCR24 inhibitor SH42 or vehicle and 3 times per week for 13 weeks *via* intraperitoneal injection. All mice were group housed under a 12-hour light-dark cycle and had free access to water and food unless indicated otherwise. All mouse experiments were reviewed by the Animal Welfare Body Leiden and executed under a license granted by the Central Authority for Scientific Procedures on Animals (CCD) under the license number AVD11600202010187 in accordance with the Dutch Act on Animal Experimentation and EU Directive 2010/63/EU. The experiments were executed at Leiden University Medical Center.

Body weight, body composition and food intake

Mice were weighed on a weighing scale, body composition was determined by an EchoMRI-100 analyzer (EchoMRI, USA), and food intake was determined by monitoring the food consumption (per cage) biweekly in experiment 1 and every 4 (or 6) weeks in experiment 2 and 3.

Plasma lipid levels

Blood was collected biweekly in experiment 1, and every 4 (or 6) weeks in experiment 2 and 3 *via* a tail vein cut after 4 hours of fasting. Plasma was obtained through centrifugation and triglyceride (TG) and total cholesterol (TC) levels were quantified using enzymatic kits (Roche Diagnostics, Germany).

In vivo plasma decay and organ uptake of triglyceride-rich lipoprotein-like particles

In experiment 1, after 6 weeks of treatment, TG-rich lipoprotein-like particles double-labeled with glycerol tri[^{3}H]oleate ([^{3}H]TO; American Radiolabeled Chemicals, USA) and [^{14}C]cholesteryl oleate ([^{14}C]CO; American Radiolabeled Chemicals, USA) were prepared as previously described[21] and injected into the tail vein of the mice (1.0 mg TG in 200 µL saline per mouse). Blood samples were drawn from the tail vein at 2, 5, 10, and 15 min after the particle injection. Subsequently, mice were killed by CO_2 inhalation and perfused with ice-cold PBS before organs were collected. Plasma samples collected following the particle injection and tissue samples that had been dissolved overnight at 55°C in Solvable (PerkinElmer, The Netherlands) were mixed with Ultima Gold liquid scintillation cocktail (PerkinElmer, The Netherlands). ^{3}H and ^{14}C activity in the samples (disintegrations per minute; dpm) were quantified using a Tri-Carb 2910TR low-activity liquid scintillation analyzer (PerkinElmer, The Netherlands). Decay of ^{3}H and ^{14}C radioactivity in plasma was expressed as the percentage of injected radioactive dose. Uptake of ^{3}H and ^{14}C radioactivity by the organs was expressed as the percentage of injected radioactive dose per gram tissue.

Desmosterol quantification

In experiment 1 and 3, after respectively 6 and 13 weeks of treatment, total desmosterol levels in the liver and plasma were quantified *via* gas chromatography-mass spectrometry (GC-MS) analysis as previously reported[22,23] with minor modifications. Briefly, 12.5 µL liver homogenates (~2.5 mg tissue) or 5-10 µL plasma samples were mixed with 70 µL ethanol and 10 µL internal standard mixture containing 20 µg/mL desmosterol-d6 (Avanti Polar Lipids, USA) in ethanol. After adding 10 µL aqueous NaOH solution (10 M), the mixtures were flushed with nitrogen gas and then saponified for 1 hour at 70°C. Subsequently, sterols were extracted with methyl *tert*-butyl ether (Honeywell Riedel-de Haën, Germany) and dried with sodium sulfate. Next, the extracts were centrifuged for 5 min at 10,000 rcf and the supernatants were dried with nitrogen gas. Finally, the samples were reconstituted in a mixture of *N*-methyl-*N*-trimethylsilyl-trifluoroacetamide (Macherey-Nagel, Germany) containing 1% Chlorotrimethylsilane (ThermoFisher, USA) and *N*-trimethylsilyl-imidazole (Sigma Aldrich, USA). An Agilent 8890 GC system coupled with an Agilent 5977B MS was used for desmosterol quantification. The injector was held at 300°C and 1 µL sample was injected splitless. Sterols were separated on a VF-5ms column (30 m × 0.25 mm × 0.25 µm) using the following temperature gradient: 1 min at 50°C, linear increase at 50°C/min to

260°C, linear increase at 4°C/min to 310°C, held for 2.3 min at 310°C. Helium was used as carrier gas at a constant flow rate of 1.40 mL/min. The transfer line was set at 280°C, the source at 230°C and the quadrupole at 150°C. The MS was operated in single ion monitoring mode (333.3 and 327.2 were used as quantifiers for desmosterol-d6 and desmosterol, respectively). Desmosterol was quantified using external calibration.

Hepatic lipid content and histology

In experiment 1, after 6 weeks of treatment, liver samples were collected and hepatic lipids were extracted from snap-frozen liver samples according to a modified protocol from Bligh and Dyer.[24] Liver TG and TC (both Roche Diagnostics, Germany) and phospholipid (PL) (Instruchemie, The Netherlands) were measured *via* enzymatic kits. Protein concentrations were measured using a BCA Protein assay kit (ThermoFisher, USA). Hepatic lipid content was expressed as nmol per mg protein. Liver samples were fixated in phosphate-buffered formaldehyde, embedded in paraffin and sectioned at 5 µm thickness. The tissue sections were stained with hematoxylin-eosin (HE) and areas of lipid accumulation (i.e., unstained areas) were quantified using ImageJ software v1.52a.

Gene expression analysis

In experiment 1, after 6 weeks of treatment, total RNA was isolated from snap-frozen liver samples with TriPure RNA Isolation Reagent (Sigma Aldrich, USA). Isolated RNA was reverse-transcribed into cDNA using Moloney murine leukemia virus reverse transcriptase (Promega, USA). Quantitative real-time PCR was performed using SYBR green (Promega, USA) on a CFX96 machine (Bio-Rad, USA). mRNA expression levels were normalized to Beta-actin (*Actb*) and glyceraldehyde-3-phosphate dehydrogenase (*Gapdh)* mRNA expression and expressed as fold change compared with the vehicle group using the ΔΔCt method. The primer sequences are listed in Supplemental Table **S1**.

Hepatic LDL receptor protein level

In experiment 1, after 6 weeks of treatment, liver samples were collected and lysed in Radioimmunoprecipitation assay buffer (ThermoFisher, USA) containing protease and phosphatase inhibitor (ThermoFisher, USA), and protein was extracted as described previously.[25] Protein concentration in the lysate was determined using a BCA Protein assay kit (ThermoFisher, USA). Subsequently, Western blots for LDLR and GAPDH were performed separately in 25 capillary cartridges (ProteinSimple, USA) according to the 12–230 kDa Jess and Wes Separation Module protocol. In short, the protein samples mixed with a fluorescent master mix were heated at 95°C for 5 min. Protein samples, goat IgG anti-mouse LDLR (R&D System, USA) or rabbit IgG anti-mouse GAPDH (Cell Signaling, USA), and anti-goat or anti-rabbit secondary antibodies (ProteinSimple, USA) were then loaded in Wes assay plates according to the kit manual instructions. The separation and immunodetection of LDLR and

GAPDH proteins were performed by the Wes Western blotting system and the results were analyzed by Compass for Simple Western v4.0.0 (ProteinSimple, USA). Data are shown as fold change from control.

Blood leukocyte isolation and flow cytometry analysis

In experiment 2, after 15 weeks of treatment, 8 mice per group were selected, based on having body weight, lean mass and fat mass close to the group mean, and 12-hour-fasted blood was collected from the retro-orbital plexus just after the mice were killed by CO_2 inhalation. In experiment 3, after 12 weeks of treatment, 4-hour-fasted blood was collected *via* a tail vein cut. Obtained blood samples were lysed for 20 min at room temperature using an erythrocyte lysis/fixation solution (BD Biosciences, USA). Leukocytes were then centrifuged at 596 rcf for 5 minutes at 4°C, reconstituted in PBS, and washed three times in PBS. Isolated leukocytes were treated with a cocktail of antibodies (details are provided in Supplemental Table **S2** and **S3**) in PBS containing 2 mM EDTA, 0.5% BSA, True-Stain monocyte blocker (Biolegend, USA) and Brilliant Stain Buffer Plus (BD Biosciences, USA) for 30 minutes at 4°C, as previously reported.[26] After staining, samples were analyzed by spectral flow cytometry using a Cytek Aurora Spectral flow cytometer (Cytek Biosciences, The Netherlands) or a Cytoflex S (Beckman Coulter, Woerden, the Netherlands). SpectroFlo v3.0 (Cytek Biosciences, The Netherlands) and FlowJoTM v10.8 software (BD Biosciences, USA) were used for spectral unmixing of the flow cytometry data and gating of the data, respectively. A representative gating strategy is shown in Supplemental Fig. **S3** and **S4**.

Atherosclerosis quantification

In experiment 2 and 3, after respectively 15 and 13 weeks of treatment, hearts were collected, fixed in phosphate-buffered formaldehyde, and embedded in paraffin. After cross-sectioning (5 µm) throughout the aortic root area, 4 consecutive sections per heart in 50 µm intervals starting at the opening of the aortic valves were used for the quantification of atherosclerotic lesions. Cross-sections were stained with hematoxylin-phloxine-saffron (HPS) to determine lesion areas. According to the guidelines of the American Heart Association adapted for mice,[27] lesions were categorized into mild lesions (type I-III, with foam cells in the intima/media or/and the presence of a fibrotic cap) or severe lesions (type IV-V, with fibrosis and progressive lesion infiltrating into the media or/and the presence of cholesterol clefs/mineralization/necrosis). Smooth muscle cells were stained using an anti-α-actin antibody (Dako, Denmark) and a secondary antibody EnVision System-HRP Labeled Polymer (Dako, Denmark) that was visualized by Liquid DAB + Substrate Chromogen System (Dako, Denmark). Collagen was stained with Sirius Red (Sigma Aldrich, USA). Macrophages were stained with an anti-Mac-3 antibody (BD Pharmingen, USA), an HRP-labeled secondary antibody and a peroxide substrate (Vector Laboratories, USA). In experiment 3, Intercellular adhesion molecule 1 (ICAM-1) area was stained using an anti-ICAM-1 antibody (Sino

Biological, USA) and a secondary antibody EnVision System-HRP Labeled Polymer (Dako, Denmark) that was visualized by Liquid DAB + Substrate Chromogen System (Dako, Denmark). Lesion areas and the areas of smooth muscle cells, collagen, macrophages and ICAM-1 were quantified using ImageJ software v1.52a.

Genetic association with coronary artery disease in humans

We used summary statistics from the genome-wide association study (GWAS) of the combined cross-ancestry meta-analysis on CAD published by Aragam *et al*.[28] which compiles data from 181,522 CAD patients among 1,165,690 participants. The data were downloaded from the GWAS catalog (https://www.ebi.ac.uk/gwas/publications/36474045). Genetic associations within the *DHCR24* locus were plotted with LocusZoom.[29]

Quantification and statistical analysis

Data were analyzed by GraphPad Prism Software, v9.3. Differences between the two groups were compared using unpaired two-tailed Student's t-tests for parametric data or Mann Whitney U test for nonparametric data. For experiments involving repeated measurements in the same animal, two-way repeated-measures ANOVA and Bonferroni post hoc analyses were performed. Data are shown as mean ± SEM. $P < 0.05$ was considered significant.

Results

SH42 increases desmosterol levels in the liver and plasma without affecting plasma lipid levels in APOE*3-Leiden.CETP mice

The E3L.CETP mouse is a well-established model of human-like lipoprotein metabolism in which females develop more pronounced hypercholesterolemia and atherosclerosis than males on a Western-type diet,[30,31] so we used female E3L.CETP mice in this study. We first evaluated the efficacy of the DHCR24 inhibitor SH42 to increase the levels of desmosterol in these mice fed a Western-type diet after 6 weeks of treatment (Fig. **1A**). As expected, SH42 remarkably elevated the desmosterol levels in the liver (137-fold; Fig. **1B**) and plasma (9.7-fold; Fig. **1C**). Throughout the study, SH42 treatment did not affect food intake (Fig. **1D**), body weight (Fig. **1E**), body fat mass (Fig. **1F**) and lean mass (Fig. **1G**), or the weight of metabolic organs including adipose tissue depots collected at the end of the study (Fig. **1H**). In line with the notion that desmosterol does not activate SREBP,[14] treatment with SH42 did not affect plasma TG (Fig. **1I**) or TC (Fig. **1J**). Meanwhile, a decrease in plasma TC (Fig. **1J**) was observed after 6 weeks compared to the baseline, regardless of treatment. This may be the outcome of self-regulation as the mice progressively get used to the cholesterol-rich diet

and we have observed a similar fluctuation of plasma TC levels in previous studies with E3L.CETP mice fed a Western-type diet.[32-34]

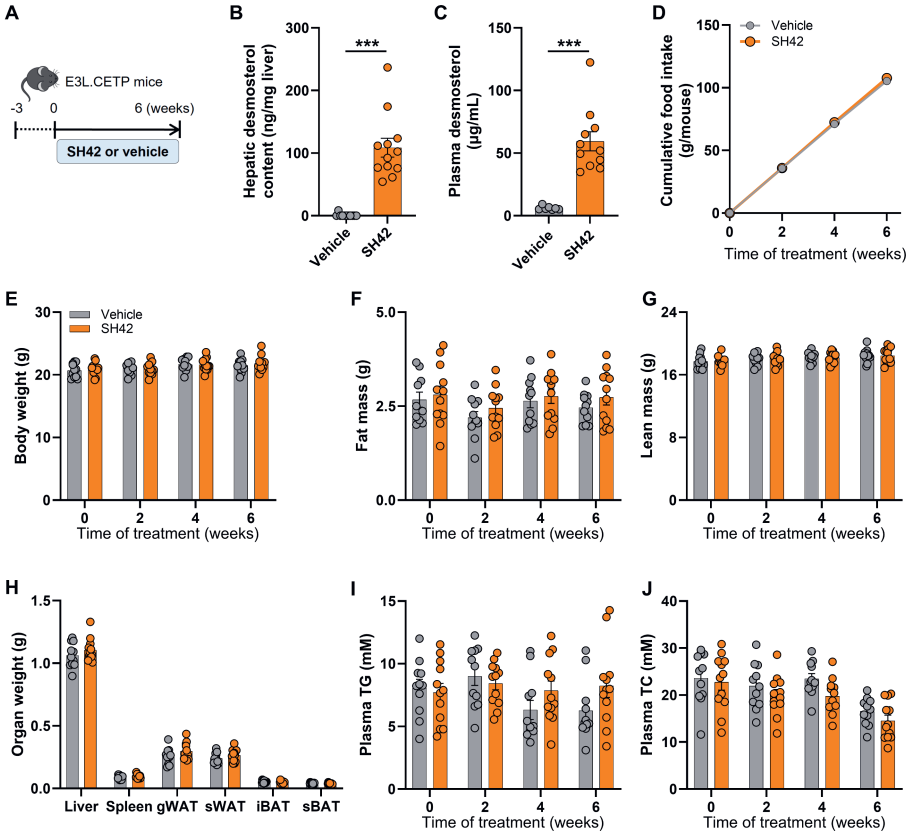

Fig. 1. DHCR24 inhibitor SH42 increases desmosterol levels in the liver and plasma without affecting plasma lipid levels in APOE*3-Leiden.CETP mice with 6 weeks of treatment. APOE*3-Leiden.CETP (E3L.CETP) mice were fed a Western-type diet containing 16% fat and 0.15% cholesterol and received intraperitoneal injections with either SH42 (0.5 mg/mouse) or vehicle 3 times per week (**A**). After 6 weeks of treatment, livers (**B**) and plasma (**C**) were collected to measure desmosterol levels. Cumulative food intake (**D**), body weight (**E**), fat mass (**F**) and lean mass (**G**) were determined every 2 weeks. After 6 weeks of treatment, the weight of various organs (**H**) was determined. Fasting plasma triglycerides (TG) (**I**) and total cholesterol (TC) (**J**) were measured every 2 weeks. gWAT, gonadal white adipose tissue; iBAT, interscapular brown adipose tissue; sBAT, subscapular brown adipose tissue; sWAT, subcutaneous white adipose tissue. Data are shown as mean ± SEM. B, C and E-J: n=7-12 mice per group; D: n=4 cages per group. B and C: data were analyzed by two-tailed Mann Whitney U test; H: data were analyzed by unpaired two-tailed Student's t-test; D-G, I and J: data were analyzed by two-way repeated-measures ANOVA and Bonferroni post hoc analysis. ***P<0.001.

SH42 reduces hepatic lipid content in APOE*3-Leiden.CETP mice

Since SH42 protects against the development of metabolic disease-associated steatotic liver diseases on a high-fat high-cholesterol diet,[17] we evaluated whether SH42 also reduces lipid accumulation in the livers of Western-type diet-fed E3L.CETP mice. While SH42 treatment did not affect liver weight (Fig. **1H**), histological analysis showed reduced lipid accumulation (-19%; Fig. **2A**). Specifically, SH42 reduced hepatic levels of TC (-30%) and PL (-9%) (Fig. **2B**). To investigate the underlying causes, we quantified the expression of hepatic genes involved in lipid metabolism. SH42 increased the gene expression of carnitine palmitoyl transferase 1 (*Cpt1*; Fig. **2C**) which is involved in fatty acid oxidation, while not altering markers of fatty acid synthesis, cholesterol synthesis, cholesterol efflux or very low-density lipoprotein production. Meanwhile, SH42 tended to decrease the protein abundance of hepatic LDLR (-19%; *P*=0.06; Fig. **2D**), which may suggest that SH42 reduces hepatic TG-rich lipoprotein remnant uptake. To test this, we intravenously injected mice with TG-rich lipoprotein-like particles labeled with glycerol tri[^{3}H]oleate ([^{3}H]TO) and [^{14}C]cholesteryl oleate ([^{14}C]CO). However, SH42 did not affect the plasma clearance of [^{3}H]TO (Fig. **2E**) or [^{14}C]CO (Fig. **2G**), or the uptake of radiolabels by the various organs including the liver (Fig. **2F, H**).

>> Fig. 2. DHCR24 inhibitor SH42 reduces hepatic lipid content without affecting the plasma decay and organ uptake of triglyceride-rich lipoprotein-like particles in APOE*3-Leiden.CETP mice. After 6 weeks of treatment, the hepatic area of lipid accumulation area (**A**) was quantified following hematoxylin-eosin (H&E) staining and hepatic lipid content (**B**) was measured. The relative mRNA expression levels of genes involved in lipid metabolism were determined in the liver (**C**). Hepatic low-density lipoprotein receptor (LDLR) protein abundance was measured (**D**). Mice were injected with triglyceride-rich lipoprotein (TRL)-like particles, double-labeled with glycerol tri[^{3}H]oleate ([^{3}H]TO) and [^{14}C]cholesteryl oleate, and the activity of ^{3}H and ^{14}C in plasma (**E**, **G**) and various tissues (**F**, **H**) was assessed. TC, total cholesterol; TG, triglycerides; PL, phospholipids; *Abca1*, ATP binding cassette subfamily A member 1; *Abcg1*, ATP binding cassette subfamily G member 1; *Acc1*, acetyl coenzyme A carboxylase 1; *Apob*, apolipoprotein B; *Cpt1*, carnitine palmitoyl transferase 1; *Fasn*, fatty acid synthase; *Fdft1*, farnesyl-diphosphate farnesyltransferase 1; *Fdps*, farnesyl diphosphate synthetase; *Hmgcr*, 3-hydroxy-3-methylglutaryl coenzyme A; *Lss*, lanosterol synthase; *Mttp*, microsomal triglyceride transfer protein; *Ppara*, peroxisome proliferator-activated receptor alpha; *Sqle*, squalene epoxidase; *Srebf1c*, sterol regulatory element-binding factor 1c; *Srebf2*, sterol regulatory element-binding factor 2; gWAT, gonadal white adipose tissue; iBAT, interscapular brown adipose tissue; sBAT, subscapular brown adipose tissue; sWAT, subcutaneous white adipose tissue. Data are shown as mean ± SEM. n=10-12 mice per group. A-D, F and H: data were analyzed by unpaired two-tailed Student's t-test; E, G: data were analyzed by two-way repeated-measures ANOVA. **P*<0.05, ***P*<0.01, ****P*<0.001.

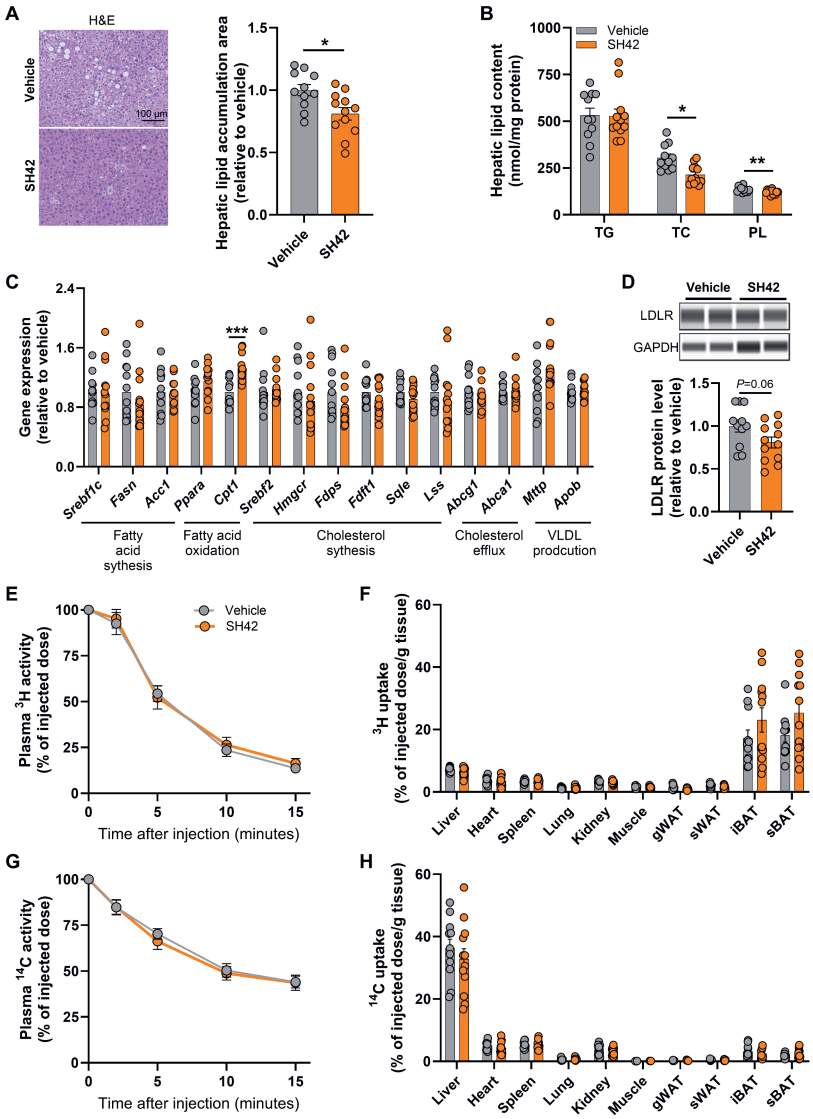

SH42 does not affect the population of circulating monocytes or atherosclerosis development in APOE*3-Leiden.CETP mice

To investigate whether SH42 reduces atherosclerosis development, E3L.CETP mice were treated with SH42 or vehicle for 15 weeks (Fig. **3A**). Throughout the study, SH42 treatment did not affect food intake (Fig. **S1A**), body weight (Fig. **S1B**), body fat mass (Fig. **S1C**) and lean mass (Fig. **S1D**), or plasma TG (Fig. **S1F**) and TC (Fig. **S1G**), and only slightly increased the weight of subscapular brown adipose tissue (sBAT; Fig. **S1E**). As the macrophages in atherosclerosis lesions are primarily derived from circulating monocytes infiltrating the

plaque,[35] we evaluated the effects of SH42 on circulating monocytes. However, the relative abundance of circulating monocytes (Fig. **3B**) and monocyte subsets (Fig. **3C**) were not affected by SH42 treatment. Next, the aortic root of the heart was stained with HPS to assess the size of the atherosclerotic lesions (Fig. **3D**). We did not observe obvious effects of SH42 treatment on atherosclerotic lesion area (Fig. **3E**) or severity (Fig. **3F**). Immunohistochemical staining of specific markers expressed in the atherosclerotic plaque revealed that lesion composition was also not affected with respect to the areas of smooth muscle cells, collagen and macrophages (Fig. **3G-J**), and no difference in the lesion stability index was observed (Fig. **3K**). These data demonstrate that SH42 does not affect atherosclerosis development in E3L.CETP mice.

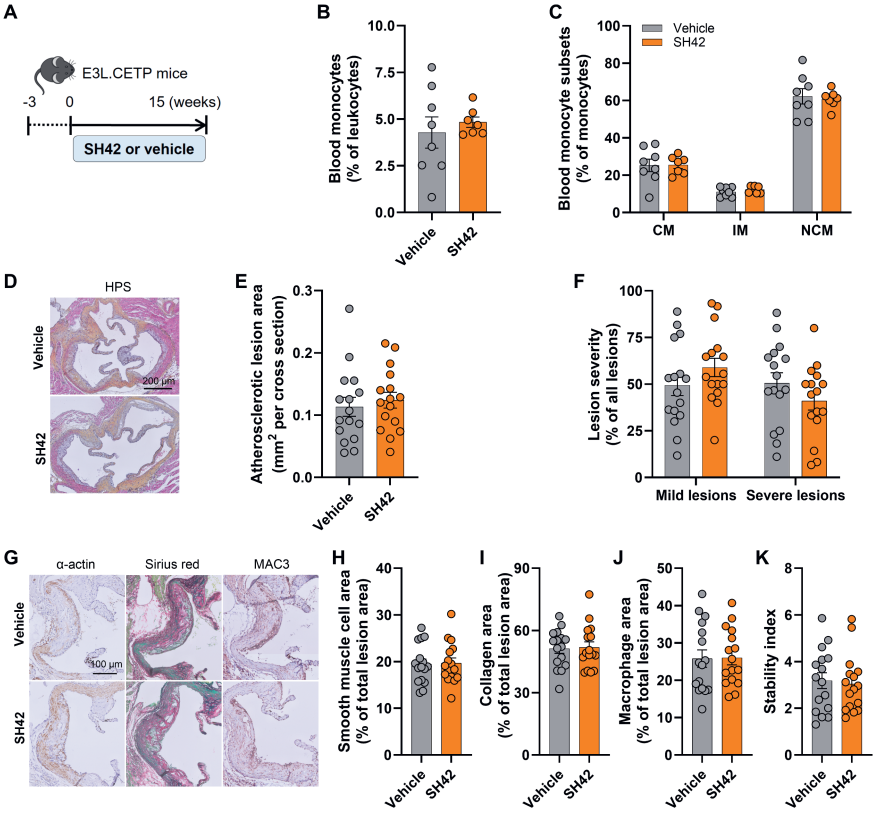

Fig. 3. DHCR24 inhibitor SH42 does not affect the population of circulating monocytes or atherosclerosis development in APOE*3-Leiden.CETP mice with 15 weeks of treatment. APOE*3-Leiden.CETP (E3L.CETP) mice were fed a Western-type diet containing 16% fat and 0.15% cholesterol and received intraperitoneal injections with either SH42 (0.5 mg/mouse) or vehicle 3 times per week (**A**). After 15 weeks of treatment, blood monocytes (**B**) and their subsets (**C**) were quantified. Hearts were collected, the aortic root valve areas were stained with hematoxylin-phloxine-saffron (HPS), and representative pictures are shown (**D**). The atherosclerotic lesion area (**E**) was determined and lesions

were categorized according to lesion severity (**F**). The smooth muscle cell (**H**), collagen (**I**) and macrophage (**J**) areas of the lesions were determined by staining with an anti-α-actin antibody, Sirius Red and anti-MAC3 antibody, respectively. Representative pictures are shown (**G**). The lesion stability index (smooth muscle cell area and collagen area/macrophage area of the lesions) was calculated (**K**). CM, classical monocyte; IM, intermediate monocyte; NCM, nonclassical monocyte. Data are shown as mean ± SEM. B, C: n=7-8 mice per group; E, F and H-K: n=16 mice per group. Data were analyzed by unpaired two-tailed Student's t-test.

SH42 increases desmosterol levels in the liver and plasma without affecting plasma lipid levels in LDL receptor knockout mice

Since atherosclerosis development in E3L.CETP mice fed a Western-type diet is mainly lipid-driven, we next assessed the effects of SH42 treatment on atherosclerosis development in LDLr-KO mice, a typical model for inflammation-driven atherosclerosis studies.[18] Given that males develop more inflamed plaques compared to females on an atherogenic diet,[36] male LDLr-KO mice were used in this study, and fed a Western-type diet and treated with SH42 or vehicle for 13 weeks (Fig. **4A**). Also in LDLr-KO mice, SH42 treatment induced a robust increase in desmosterol levels in the liver (29-fold; Fig. **4B**) and plasma (7.4-fold; Fig. **4C**) without affecting food intake (Fig. **4D**), body weight (Fig. **4E**), body fat mass (Fig. **4F**) and lean mass (Fig. **4G**), or the weight of several organs (Fig. **4H**). Throughout the treatment period, SH42 did not affect the plasma levels of TG (Fig. **4I**) or TC (Fig. **4J**).

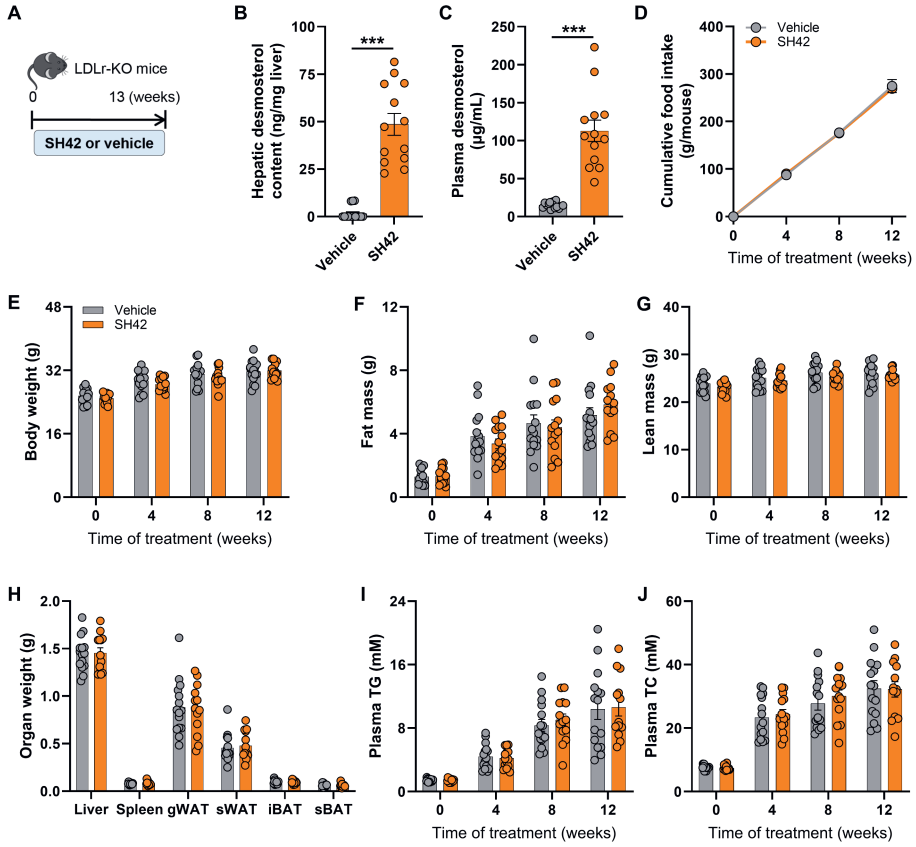

Fig. 4. DHCR24 inhibitor SH42 increases desmosterol levels in the liver and plasma without affecting plasma lipid levels in LDL receptor knockout mice with 13 weeks of treatment. LDL receptor knockout (LDLr-KO) mice were fed a Western-type diet containing 16% fat and 0.25% cholesterol and received intraperitoneal injections with either SH42 (0.5 mg/mouse) or vehicle 3 times per week (**A**). After 13 weeks of treatment, mice were killed, and livers (**B**) and plasma (**C**) were collected to measure desmosterol levels. Cumulative food intake (**D**), body weight (**E**), fat mass (**F**) and lean mass (**G**) were determined every 4 weeks. After 13 weeks of treatment, the weight of various organs (**H**) was determined. Fasting plasma triglycerides (TG) (**I**) and total cholesterol (TC) (**J**) were measured every 4 weeks. gWAT, gonadal white adipose tissue; iBAT, interscapular brown adipose tissue; sBAT, subscapular brown adipose tissue; sWAT, subcutaneous white adipose tissue. Data are shown as mean ± SEM. B, C and E-J: n=13-15 mice per group; D: n=6-7 cages per group. B and C: data were analyzed by two-tailed Mann Whitney U test; H: data were analyzed by unpaired two-tailed Student's t-test; D-G, I and J: data were analyzed by two-way repeated-measures ANOVA. ***P<0.001.

SH42 decreases circulating non-classical monocytes without affecting atherosclerosis development in LDL receptor knockout mice

In LDLr-KO mice, SH42 tended to decrease the relative abundance of total circulating monocytes (-24%; P=0.06; Fig. **5A**) and intermediate monocytes (IM, -17%; P=0.06) and

significantly decreased the proportion of non-classical monocytes (NCM; -17%) (Fig. **5B**). Nonetheless, SH42 treatment did not affect the atherosclerotic lesion area (Fig. **5C**, **D**) or lesion severity (Fig. **5E**). The area of ICAM-1 (Fig. **5F**, **G**) was not altered by SH42 treatment. Immunohistochemical stainings of specific markers expressed in the atherosclerotic plaque were performed to reveal the lesion composition (Fig. **5H**). Interestingly, SH42 treatment did increase the relative smooth muscle cell area (+72%; Fig. **5I**) in the atherosclerotic lesions but as the lesion collagen area (Fig. **5J**) and macrophage area (Fig. **5K**) were not affected, the lesion stability index (Fig. **5L**) was unchanged by SH42 treatment. These data suggest that even though SH42 did regulate the population of circulating monocytes in LDLr-KO mice, it did not attenuate atherosclerosis development.

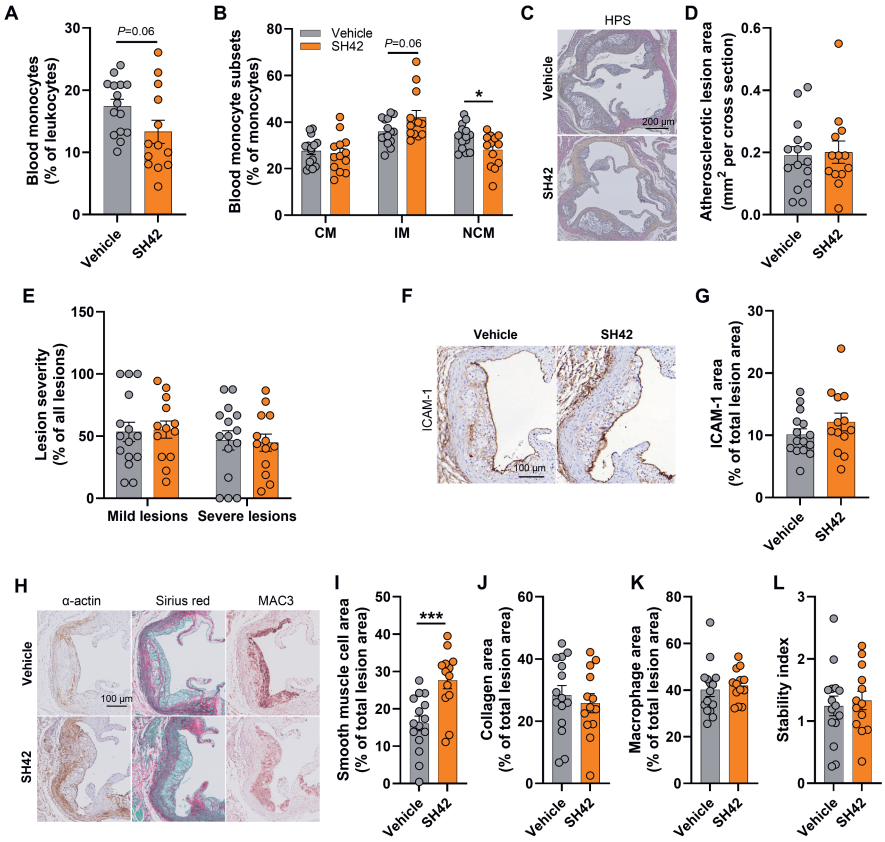

Fig. 5. DHCR24 inhibitor SH42 decreases circulating non-classical monocytes without affecting atherosclerosis development in LDL receptor knockout mice. After 13 weeks of treatment, mice were killed and the relative number of blood monocytes (**A**) and their subsets (**B**) were quantified. Hearts were collected, the aortic root valve areas were stained with hematoxylin-phloxine-saffron (HPS), and representative pictures are shown (**C**). The atherosclerotic lesion area (**D**) was determined and lesions were categorized according to lesion severity (**E**). Intercellular adhesion molecule 1 (ICAM-1) area (**G**) in lesions was stained using an anti-ICAM-1 antibody. Representative pictures are shown (**F**). The smooth muscle cell (**I**), collagen (**J**) and macrophage (**K**) areas of the lesions were determined by

staining aortic root lesions with an anti-α-actin antibody, Sirius Red and anti-MAC3 antibody, respectively. Representative pictures are shown (**H**). The stability index (smooth muscle cell area and collagen area/macrophage area of the lesions) was calculated (**L**). CM, classical monocyte; IM, intermediate monocyte; NCM, nonclassical monocyte. Data are shown as mean ± SEM. n=13-15 mice per group. Data were analyzed by unpaired two-tailed Student's t-test. **P*<0.05, ***P*<0.01.

Genetic association of *DHCR24* variants with coronary artery disease in humans

Since DHCR24 inhibition by SH42 did not affect atherosclerosis in both mouse models, we next evaluated whether common genetic variants within the *DHCR24* locus would associate with coronary artery disease (CAD) in humans using the largest dataset published to date.[28] When querying the entire *DHCR24* locus (chr1.p32.3, 500 kb up and downstream of *DHCR24*), we could observe variants very strongly associated with CAD (Fig. **S2**, upper panel). However, the *DHCR24* locus encompasses the proprotein convertase subtilisin/kexin type 9 (*PCSK9*) gene (~150 kb downstream of *DHCR24*), one of the most closely related loci with LDL cholesterol levels and CAD in humans (Fig. **S2**, upper panel). Although functional evidence does not support the association of *Dhcr24* with atherosclerosis in mice and that no variant reaches significance (*P*=5.0E-8) in the genomic region of *DHCR24 per se* in humans (Fig. **S2**, lower panel), we cannot state with certainty that there is no genetic association between the *DHCR24* locus and CAD in humans.

Discussion

LXR activation in macrophages is a potential strategy to attenuate atherosclerosis development, but currently available synthetic LXR agonists also stimulate lipogenesis in hepatocytes *via* the activation of SREBP,[7-11] based on which their clinical development has failed. Interestingly, desmosterol has been reported to selectively activate LXR in macrophages without inducing lipogenesis.[13,14] In the present study, we investigated the effects of desmosterol accumulation induced by SH42, a specific DHCR24 inhibitor, on lipid metabolism and atherosclerosis development in both E3L.CETP mice and LDLr-KO mice. We demonstrated that SH42 robustly increases the desmosterol levels in the liver and plasma in both mouse models, accompanied by a reduction in hepatic lipids as shown in E3L.CETP mice, and an improved regulation of circulating monocyte populations as shown in LDLr-KO mice, albeit without affecting atherosclerosis development in either model.

First, we observed that SH42 largely increases desmosterol levels in the liver and plasma. Other DHCR24 inhibitors, in addition to inducing accumulation of desmosterol, like DMHCA and triparanol, also induce accumulation of other intermediates of cholesterol biosynthesis, including zymosterol and lathosterol,[15,37] and at least the latter has been reported to

negatively correlate with the risk of cardiovascular diseases.[38] SH42 has been shown to primarily induce a robust accumulation of desmosterol.[15] Therefore, it is convincing that the effects of SH42 in this study were from the accumulated desmosterol, instead of other sterols. With the elevated desmosterol levels, we observed a reduction in hepatic lipids as shown in E3L.CETP mice and unaltered plasma lipids in both mouse models. The fact that the increase in the endogenous LXR agonist desmosterol does not induce hepatosteatosis or dyslipidemia is in favorable contrast to the effects of synthetic LXR agonists that stimulate excessive lipogenesis in hepatocytes.[10,11] In line with the selective activation of LXR in macrophages,[14] SH42 did not change the overall hepatic expression of lipogenic genes in E3L.CETP mice. These data also support our previous observations that SH42 does not induce lipogenesis in E3L.CETP mice fed a high-fat high-cholesterol diet to induce metabolic dysfunction-associated steatohepatitis, and in fact markedly reduces both liver steatosis and inflammation.[17] Interestingly, the expression of hepatic *Cpt1* which is involved in fatty acid oxidation was decreased by SH42 treatment. The effect of SH42/desmosterol on fatty acid oxidation has not been investigated in detail. Given that the interaction between fatty acid and cholesterol metabolism has been widely reported[39,40] and increasing hepatic cholesterol by dietary cholesterol supplementation has been shown to reduce *Cpt1* expression, we speculate that the upregulated *Cpt1* may be connected to the decreased hepatic cholesterol levels following SH42 treatment in this study. While desmosterol accumulation in macrophages upon SH42 treatment has previously been described to upregulate the expression of the LXR target genes *Abcg1* and *Abca1* that encode cholesterol transporters,[14,41] we did not observe altered *Abcg1* and *Abca1* gene expression in the liver here. This may be explained by the modest contribution of monocytes and macrophages to the total cell count in the liver, with hepatocytes predominating.

It is well-established that intracellular cholesterol levels can determine hepatic LDLR expression through a negative feedback mechanism.[42-44] Surprisingly, a decrease in hepatic cholesterol was observed in E3L.CETP mice coincided with a tendency towards decreased hepatic LDL receptor protein abundance with SH42 treatment. Some studies have demonstrated that desmosterol may partly replace cholesterol in certain physiological processes.[45,46] A study found that desmosterol has a regulatory feedback role and can reduce LDL receptor protein levels, in a manner similar to that of supplementary cholesterol.[47] Thus, accumulated desmosterol by SH42 treatment may decrease the abundance of LDL receptors. This also suggests that SH42 may reduce the LDL receptor-mediated hepatic uptake of ApoE-containing TG-rich lipoprotein remnants. However, SH42 did not decrease the hepatic uptake of radioactively labeled TG-rich lipoprotein-like particles in this study. Of note, the kinetic study with radiolabeled particles was performed 4 hours after the last dosing of SH42, possibly missing a significant effect on hepatic lipoprotein remnant uptake. Nonetheless, the fact that SH42 increases desmosterol levels by blocking its conversion into cholesterol seems to be the most likely reason for the decrease in hepatic

cholesterol content, while this effect is not strong enough to influence circulating cholesterol levels, especially in the context of a cholesterol-rich diet. Taken together, DHCR24 inhibition by SH42 does not induce hepatic lipogenesis and in fact lowers hepatic cholesterol, presumably as a consequence of macrophage-specific LXR activation and generally lowered cholesterol synthesis.

While we previously showed that SH42 was very effective in attenuating experimental peritonitis[16] and metabolic dysfunction-associated steatohepatitis,[17] we did not observe an effect of SH42 treatment on atherosclerotic lesion area, severity or markers of plaque stability either in E3L.CETP mice, a model for lipid-driven atherosclerosis, or in LDLr-KO mice, a model of inflammation-driven atherosclerosis. This was quite surprising, as desmosterol depletion induced by overexpression of DHCR24 in myeloid cells in male LDLr-KO mice fed a diet containing 21% fat and 1.25% cholesterol was demonstrated to aggravate atherosclerosis by increasing macrophage-driven inflammation.[41] Circulating monocytes and monocyte subsets usually strongly correlate with atherosclerotic progression in mice and humans.[48,49] Although the exact roles of monocyte subtypes in atherosclerosis development are still under debate,[50,51] NCMs and IMs have been described as more inflammatory than CMs due to their higher pro-inflammatory cytokine production.[52,53] In this study, while CM levels were unaffected, SH42 reduced the proportion of circulating NCMs in LDLr-KO mice where IMs tended to be increased. However, the area of ICAM-1 which is responsible for the recruitment of circulating monocytes in atherosclerotic lesions was not affected. Interestingly, SH42 treatment largely increased the lesion content of smooth muscle cells that contribute to stabilizing the plaque by generating the extracellular matrix and supporting the development of fibrous caps.[54] Nonetheless, the lesion stability index was overall not altered due to unchanged macrophage and collagen content of the lesions. Here, it may be possible that we did not obtain a sufficiently high level of desmosterol specifically in macrophages within atherosclerotic plaques to exert a measurable effect on atherosclerosis development. Also, it has been described that in the transition from macrophage to foam cell, DHCR24 is strongly suppressed.[13] This could explain why no added benefits of DHCR24 inhibition were observed in the current study.

As mentioned in the result section, the proximity of *DHCR24* and *PCSK9* at the same locus does not rule out a genetic association between *DHCR24* variants locus and CAD in humans. Future studies should thus be performed in humans to investigate the association between *DHCR24* variation and desmosterol levels, and between desmosterol levels and CAD.

In summary, we demonstrated that the DHCR24 inhibitor SH42 induces a profound increase in desmosterol levels in both E3L.CETP mice and LDLr-KO mice without stimulation of lipogenesis or aggravating hyperlipidemia, and even reduces hepatic lipids as shown in E3L.CETP mice. Desmosterol accumulation through SH42 treatment has stronger effects on

blood monocyte populations and atherosclerotic lesion composition in LDLr-KO mice than in E3L.CETP mice but in neither mouse model ameliorates atherosclerotic progression.

Limitations of the study

Firstly, while SH42 has been reported to enhance LXR activation in macrophages, we were unable to evaluate the effect of SH42 on monocytes/macrophages that reside within the lesions in our study due to technical limitations associated with the flow cytometry used to characterize the macrophage subpopulations. Secondly, we observed that SH42 decreases hepatic lipid content, the underlying mechanism of which was not fully elucidated. It is worth exploring the potential therapeutic effects of SH42 on lipid-driven liver diseases such as metabolic dysfunction-associated steatohepatitis further.

Acknowledgments

This work was supported by the Novo Nordisk Foundation (grant NNF18OC0032394 to M.S.), The Netherlands Cardiovascular Research Initiative CVON-GENIUS-2 (grant to P.C.N.R.), the Rembrandt Institute of Cardiovascular Science (grant to S.K.) and the Chinese Scholarship Council (grant 202006850007 to X.G.). The authors thank Amanda Pronk, Reshma Lalai, Trea Streefland, Salwa Afkir, Hetty Sips and Matz Mulderij (Division of Endocrinology, Department of Medicine, LUMC, Leiden, The Netherlands) for their excellent technical assistance.

Author contributions

Conceptualization: X.G., E.Z., B.S., B.G., M.G., S.K., Y.W., P.C.N.R. and M.S.; Data curation: X.G., S.K., Y.W., P.C.N.R. and M.S.; Formal analysis: X.G., B.S., J.L., C.A., M.H., and A.R.; Investigation: X.G., Z.Y., C.A., B.S., J.L., M.H., A.R., and M.S.; Resources: J.K., B.G., M.G., C.M., F.B., P.C.N.R. and M.S.; Writing – original draft: X.G.; Writing – review & editing: X.G., P.C.N.R. and M.S.; Supervision: Y.W., P.C.N.R. and M.S.; Funding acquisition: X.G., S.K., P.C.N.R and M.S.

Declaration of interests

The authors declare no competing interests.

STAR METHODS

RESOURCE AVAILABILITY

Lead contact

Further information and requests for resources should be directed to and will be fulfilled by the lead contact, Milena Schönke (m.schoenke@lumc.nl).

Materials availability

This study did not generate unique reagents.

Data and code availability

- All data reported in this paper will be shared by the lead contact upon request.
- No new code was generated in this study.
- Any additional information required to reanalyze the data reported in this paper is available from the lead contact upon request.

References

1. World Health Organization. Cardiovascular diseases (CVDs). https://www.who.int/news-room/fact-sheets/detail/cardiovascular-diseases-(cvds). (2021).
2. McLaren J. E., Michael D. R., Ashlin T. G.*, et al.* Cytokines, macrophage lipid metabolism and foam cells: Implications for cardiovascular disease therapy. *Prog. Lipid Res.* **50**, 331–347 (2011).
3. Calkin A. C., Tontonoz P. Liver x receptor signaling pathways and atherosclerosis. *Arterioscler. Thromb. Vasc. Biol.* **30**, 1513–1518 (2010).
4. Endo-Umeda K., Kim E., Thomas D. G.*, et al.* Myeloid LXR (Liver X Receptor) Deficiency Induces Inflammatory Gene Expression in Foamy Macrophages and Accelerates Atherosclerosis. *Arterioscler. Thromb. Vasc. Biol.* **42**, 719–731 (2022).
5. Varin A., Thomas C., Ishibashi M.*, et al.* Liver X receptor activation promotes polyunsaturated fatty acid synthesis in macrophages: relevance in the context of atherosclerosis. *Arterioscler. Thromb. Vasc. Biol.* **35**, 1357–1365 (2015).
6. Naik S. U., Wang X., Da Silva J. S.*, et al.* Pharmacological activation of liver X receptors promotes reverse cholesterol transport in vivo. *Circulation* **113**, 90–97 (2006).
7. Schultz J. R., Tu H., Luk A.*, et al.* Role of LXRs in control of lipogenesis. *Genes Dev.* **14**, 2831–2838 (2000).
8. Yuan W., Yu B., Yu M.*, et al.* Synthetic high-density lipoproteins delivering liver X receptor agonist prevent atherogenesis by enhancing reverse cholesterol transport. *J. Control. Release* **329**, 361–371 (2021).
9. Kappus M. S., Murphy A. J., Abramowicz S.*, et al.* Activation of liver X receptor decreases atherosclerosis in Ldlr^{-}/$^{-}$ mice in the absence of ATP-binding cassette transporters A1 and G1 in myeloid cells. *Arterioscler. Thromb. Vasc. Biol.* **34**, 279–284 (2014).
10. Bełtowski J. Liver X receptors (LXR) as therapeutic targets in dyslipidemia. *Cardiovasc. Ther.* **26**, 297–316 (2008).
11. Faulds M. H., Zhao C., Dahlman-Wright K. Molecular biology and functional genomics of liver X receptors (LXR) in relationship to metabolic diseases. *Curr. Opin. Pharmacol.* **10**, 692–697 (2010).
12. Kirchgessner T. G., Sleph P., Ostrowski J.*, et al.* Beneficial and Adverse Effects of an LXR Agonist on Human Lipid and Lipoprotein Metabolism and Circulating Neutrophils. *Cell Metab.* **24**, 223–233 (2016).
13. Spann N. J., Garmire L. X., McDonald J. G.*, et al.* Regulated accumulation of desmosterol integrates macrophage lipid metabolism and inflammatory responses. *Cell* **151**, 138–152 (2012).
14. Muse E. D., Yu S., Edillor C. R.*, et al.* Cell-specific discrimination of desmosterol and desmosterol mimetics confers selective regulation of LXR and SREBP in macrophages. *Proc. Natl. Acad. Sci. U. S. A.* **115**, E4680–e4689 (2018).
15. Müller C., Hemmers S., Bartl N.*, et al.* New chemotype of selective and potent inhibitors of human delta 24-dehydrocholesterol reductase. *Eur. J. Med. Chem.* **140**, 305–320 (2017).
16. Körner A., Zhou E., Müller C.*, et al.* Inhibition of Δ24-dehydrocholesterol reductase activates pro-resolving lipid mediator biosynthesis and inflammation resolution. *Proc. Natl. Acad. Sci. U. S. A.* **116**, 20623–20634 (2019).
17. Zhou E., Ge X., Nakashima H.*, et al.* Inhibition of DHCR24 activates LXRα to ameliorate hepatic steatosis and inflammation. *EMBO Mol. Med.*, e16845 (2023).
18. Oppi S., Lüscher T. F., Stein S. Mouse Models for Atherosclerosis Research-Which Is My Line? *Front Cardiovasc Med* **6**, 46 (2019).

19. Westerterp M., van der Hoogt C. C., de Haan W.*, et al.* Cholesteryl ester transfer protein decreases high-density lipoprotein and severely aggravates atherosclerosis in APOE*3-Leiden mice. *Arterioscler. Thromb. Vasc. Biol.* **26**, 2552–2559 (2006).
20. van Eenige R., Verhave P. S., Koemans P. J.*, et al.* RandoMice, a novel, user-friendly randomization tool in animal research. *PLoS One* **15**, e0237096 (2020).
21. Ying Z., Boon M. R., Coskun T.*, et al.* A simplified procedure to trace triglyceride-rich lipoprotein metabolism in vivo. *Physiol Rep* **9**, e14820 (2021).
22. Giera M., Plössl F., Bracher F. Fast and easy in vitro screening assay for cholesterol biosynthesis inhibitors in the post-squalene pathway. *Steroids* **72**, 633–642 (2007).
23. Müller C., Junker J., Bracher F.*, et al.* A gas chromatography-mass spectrometry-based whole-cell screening assay for target identification in distal cholesterol biosynthesis. *Nat. Protoc.* **14**, 2546–2570 (2019).
24. Bligh E. G., Dyer W. J. A rapid method of total lipid extraction and purification. *Can. J. Biochem. Physiol.* **37**, 911–917 (1959).
25. In Het Panhuis W., Kooijman S., Brouwers B.*, et al.* Mild Exercise does not prevent atherosclerosis in APOE*3-Leiden.CETP mice or improve lipoprotein profile of men with obesity. *Obesity (Silver Spring)* **28 Suppl 1**, S93–s103 (2020).
26. van der Zande H. J. P., Lambooij J. M., Chavanelle V.*, et al.* Effects of a novel polyphenol-rich plant extract on body composition, inflammation, insulin sensitivity, and glucose homeostasis in obese mice. *Int. J. Obes. (Lond.)* **45**, 2016–2027 (2021).
27. Wong M. C., van Diepen J. A., Hu L.*, et al.* Hepatocyte-specific IKKβ expression aggravates atherosclerosis development in APOE*3-Leiden mice. *Atherosclerosis* **220**, 362–368 (2012).
28. Aragam K. G., Jiang T., Goel A.*, et al.* Discovery and systematic characterization of risk variants and genes for coronary artery disease in over a million participants. *Nat. Genet.* **54**, 1803–1815 (2022).
29. Boughton A. P., Welch R. P., Flickinger M.*, et al.* LocusZoom.js: interactive and embeddable visualization of genetic association study results. *Bioinformatics* **37**, 3017–3018 (2021).
30. van Vlijmen B. J., van 't Hof H. B., Mol M. J.*, et al.* Modulation of very low density lipoprotein production and clearance contributes to age- and gender- dependent hyperlipoproteinemia in apolipoprotein E3-Leiden transgenic mice. *J. Clin. Invest.* **97**, 1184–1192 (1996).
31. van Gemert Y., Blom A. B., Di Ceglie I.*, et al.* Intensive cholesterol-lowering treatment reduces synovial inflammation during early collagenase-induced osteoarthritis, but not pathology at end-stage disease in female dyslipidemic E3L.CETP mice. *Osteoarthritis Cartilage* **31**, 934–943 (2023).
32. Zhou E., Li Z., Nakashima H.*, et al.* Beneficial effects of brown fat activation on top of PCSK9 inhibition with alirocumab on dyslipidemia and atherosclerosis development in APOE*3-Leiden.CETP mice. *Pharmacol. Res.* **167**, 105524 (2021).
33. Liu C., Schönke M., Zhou E.*, et al.* Pharmacological treatment with FGF21 strongly improves plasma cholesterol metabolism to reduce atherosclerosis. *Cardiovasc. Res.* **118**, 489–502 (2022).
34. In Het Panhuis W., Schönke M., Modder M.*, et al.* Time-restricted feeding attenuates hypercholesterolaemia and atherosclerosis development during circadian disturbance in APOE∗3-Leiden.CETP mice. *EBioMedicine* **93**, 104680 (2023).
35. Flynn M. C., Pernes G., Lee M. K. S.*, et al.* Monocytes, Macrophages, and Metabolic Disease in Atherosclerosis. *Front. Pharmacol.* **10**, 666 (2019).
36. Man J. J., Beckman J. A., Jaffe I. Z. Sex as a Biological Variable in Atherosclerosis. *Circ. Res.* **126**, 1297–1319 (2020).

37. El-Darzi N., Astafev A., Mast N.*, et al.* N,N-Dimethyl-3β-hydroxycholenamide Reduces Retinal Cholesterol via Partial Inhibition of Retinal Cholesterol Biosynthesis Rather Than its Liver X Receptor Transcriptional Activity. *Front. Pharmacol.* **9**, 827 (2018).
38. Weingärtner O., Lütjohann D., Meyer S.*, et al.* Low serum lathosterol levels associate with fatal cardiovascular disease and excess all-cause mortality: a prospective cohort study. *Clin. Res. Cardiol.* **108**, 1381–1385 (2019).
39. Tobin K. A., Steineger H. H., Alberti S.*, et al.* Cross-talk between fatty acid and cholesterol metabolism mediated by liver X receptor-alpha. *Mol. Endocrinol.* **14**, 741–752 (2000).
40. Gibbons G. F. Regulation of fatty acid and cholesterol synthesis: co-operation or competition? *Prog. Lipid Res.* **42**, 479–497 (2003).
41. Zhang X., McDonald J. G., Aryal B.*, et al.* Desmosterol suppresses macrophage inflammasome activation and protects against vascular inflammation and atherosclerosis. *Proc. Natl. Acad. Sci. U. S. A.* **118**, e2107682118 (2021).
42. Brown M. S., Goldstein J. L. The SREBP pathway: regulation of cholesterol metabolism by proteolysis of a membrane-bound transcription factor. *Cell* **89**, 331–340 (1997).
43. Brown M. S., Goldstein J. L. A proteolytic pathway that controls the cholesterol content of membranes, cells, and blood. *Proc. Natl. Acad. Sci. U. S. A.* **96**, 11041–11048 (1999).
44. Chen Z., Chen L., Sun B.*, et al.* LDLR inhibition promotes hepatocellular carcinoma proliferation and metastasis by elevating intracellular cholesterol synthesis through the MEK/ERK signaling pathway. *Mol Metab* **51**, 101230 (2021).
45. Huster D., Scheidt H. A., Arnold K.*, et al.* Desmosterol may replace cholesterol in lipid membranes. *Biophys. J.* **88**, 1838–1844 (2005).
46. Heverin M., Meaney S., Brafman A.*, et al.* Studies on the cholesterol-free mouse: strong activation of LXR-regulated hepatic genes when replacing cholesterol with desmosterol. *Arterioscler. Thromb. Vasc. Biol.* **27**, 2191–2197 (2007).
47. Rodríguez-Acebes S., de la Cueva P., Fernández-Hernando C.*, et al.* Desmosterol can replace cholesterol in sustaining cell proliferation and regulating the SREBP pathway in a sterol-Delta24-reductase-deficient cell line. *Biochem. J.* **420**, 305–315 (2009).
48. Swirski F. K., Pittet M. J., Kircher M. F.*, et al.* Monocyte accumulation in mouse atherogenesis is progressive and proportional to extent of disease. *Proc. Natl. Acad. Sci. U. S. A.* **103**, 10340–10345 (2006).
49. Tacke F., Alvarez D., Kaplan T. J.*, et al.* Monocyte subsets differentially employ CCR2, CCR5, and CX3CR1 to accumulate within atherosclerotic plaques. *J. Clin. Invest.* **117**, 185–194 (2007).
50. Narasimhan P. B., Marcovecchio P., Hamers A. A. J.*, et al.* Nonclassical Monocytes in Health and Disease. *Annu. Rev. Immunol.* **37**, 439–456 (2019).
51. Thomas G., Tacke R., Hedrick C. C.*, et al.* Nonclassical patrolling monocyte function in the vasculature. *Arterioscler. Thromb. Vasc. Biol.* **35**, 1306–1316 (2015).
52. Patel V. K., Williams H., Li S. C. H.*, et al.* Monocyte inflammatory profile is specific for individuals and associated with altered blood lipid levels. *Atherosclerosis* **263**, 15–23 (2017).
53. Mukherjee R., Kanti Barman P., Kumar Thatoi P.*, et al.* Non-Classical monocytes display inflammatory features: Validation in Sepsis and Systemic Lupus Erythematous. *Sci. Rep.* **5**, 13886 (2015).
54. Ross R. Atherosclerosis--an inflammatory disease. *N. Engl. J. Med.* **340**, 115–126 (1999).

Supplemental Materials

Supplemental tables

Table S1. Primer sequences for quantitative real-time PCR, related to Figure 2C and STAR Methods

	Primers	
Gene	Forward (5'- 3')	Reverse (5'- 3')
Abca1	CCCAGAGCAAAAAGCGACTC	GGTCATCATCACTTTGGTCCTTG
Abcg1	AGGTCTCAGCCTTCTAAAGTTCCTC	TCTCTCGAAGTGAATGAAATTTATCG
Acc1	AACGTGCAATCCGATTTGTT	GAGCAGTTCTGGGAGTTTCG
Actb	AACCGTGAAAAGATGACCCAGAT	CACAGCCTGGATGGCTACGTA
Apob	GCCCATTGTGGACAAGTTGATC	CCAGGACTTGGAGGTCTTGGA
Cpt1	GAGACTTCCAACGCATGACA	ATGGGTTGGGGTGATGTAGA
Fasn	GCGCTCCTCGCTTGTCGTCT	TAGAGCCCAGCCTTCCATCTCCTG
Fdft1	TGCCTCAGAGTTTGAAGACCCCAT	TCCTGAGGCCAAAACTTCCTTCCT
Fdps	ATGGAGATGGGCGAGTTCTTC	CCGACCTTTCCCGTCACA
Gapdh	GGGGCTGGCATTGCTCTCAA	TTGCTCAGTGTCCTTGCTGGGG
Hmgcr	CCGGCAACAACAAGATCTGTG	ATGTACAGGATGGCGATGCA
Lss	AGGAGCACGTTTCTCGGATCAA	AGGGCAGAAACTCAGGTCTGTG
Mttp	CTCTTGGCAGTGCTTTTTCTCT	GAGCTTGTATAGCCGCTCATT
Ppara	ATGCCAGTACTGCCGTTTTC	GGCCTTGACCTTGTTCATGT
Sqle	CCAACTCAATGGGTCTGTTCCT	TGGCTTAGCAAAGTCTTCCAACT
Srebf1c	AGCCGTGGTGAGAAGCGCAC	ACACCAGGTCCTTCAGTGATTTGCT
Srebf2	TGAAGCTGGCCAATCAGAAAA	ACATCACTGTCCACCAGACTGC

Abca1, ATP binding cassette subfamily A member 1; *Abcg1*, ATP binding cassette subfamily G member 1; *Acc1*, acetyl coenzyme A carboxylase 1; *Actb*, Beta-actin; *Apob,* apolipoprotein B; *Cpt1*, carnitine palmitoyl transferase 1; *Fasn*, fatty acid synthase; *Fdft1*, farnesyl-diphosphate farnesyltransferase 1; *Fdps*, farnesyl diphosphate synthetase; *Gapdh*, glyceraldehyde-3-phosphate dehydrogenase; *Hmgcr*, 3-hydroxy-3-methylglutaryl coenzyme A; *Lss*, lanosterol synthase; *Mttp*, microsomal triglyceride transfer protein; *Ppara*, peroxisome proliferator-activated receptor alpha; *Sqle*, squalene epoxidase; *Srebf1c*, sterol regulatory element-binding factor 1c; *Srebf2*, sterol regulatory element-binding factor 2.

Table S2. Antibodies used for flow cytometry in blood leukocytes of APOE*3-Leiden.CETP mice, related to Figure 3C

Target	Clone	Conjugate	Source	Catalog number
CD3	17A2	BV605	Biolegend	100237
CD11b	M1/70	PE-Cy7	eBioscience	25-0112-82
CD19	MB19-1	FITC	eBioscience	11-0191-85
CD45	30-F11	BV785	Biolegend	103149
Ly6C	HK1.4	BV510	Biolegend	128033
Ly6G	1A8	Spark Blue 550	Biolegend	127664
NK1.1	PK136	PerCP-Cy5.5	Biolegend	108727
Siglec-F	E50-2440	BV480	BD Biosciences	746668

Table S3. Antibodies used for flow cytometry in blood leukocytes of LDL receptor knockout mice, related to Figure 5B

Target	Clone	Conjugate	Source	Catalog number
CD11b	M1/70	BV420	Biolegend	101251
CD19	eBio1D3	Pe	eBioscience	12-0193-83
Fixable Viability Dye	NA	eFluor780	eBioscience	15383562
Ly6C	HK1.4	APC	eBioscience	17-59432-82
Ly6G	D7	FITC	Biolegend	108106
NK1.1	PK136	BV650	BD Horizon	564143
Thy1.2	53-2.1	Pe-Cy	Biolegend	140324

Supplemental figures

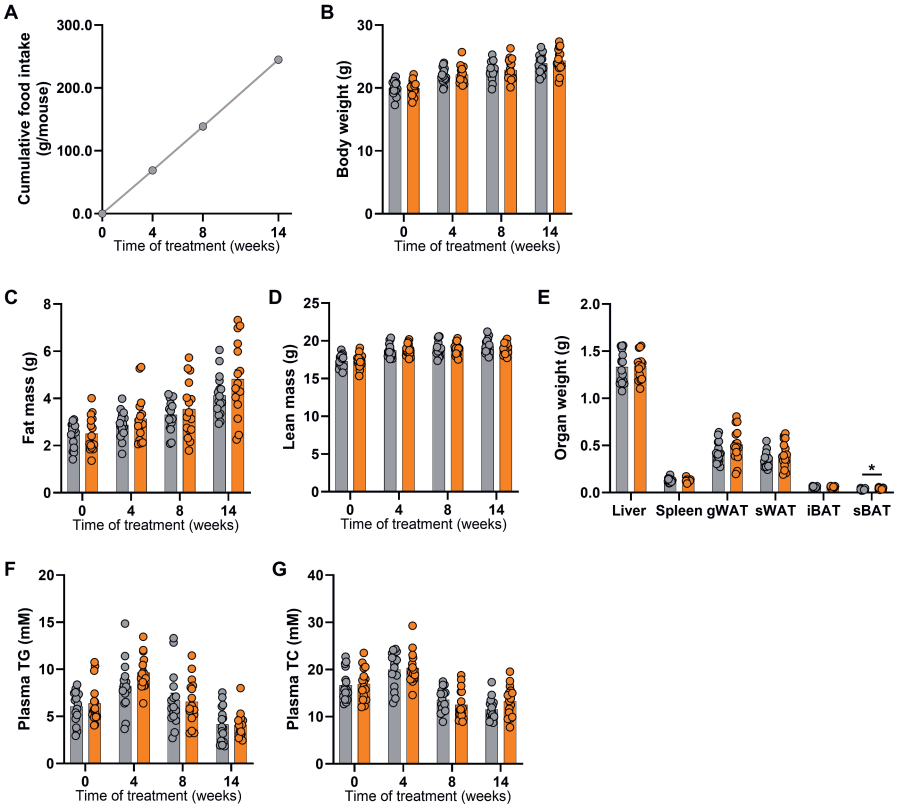

Fig. S1. DHCR24 inhibitor SH42 does not affect the body weight, body composition or plasma lipid levels in APOE*3-Leiden.CETP mice with 15 weeks of treatment, related to Figure 3. Throughout 15 weeks of treatment, cumulative food intake (**A**), body weight (**B**), fat mass (**C**) and lean mass (**D**) were determined at week 4, 8 and 14. After 15 weeks of treatment, the weight of various organs (**E**) was determined. Fasting plasma triglycerides (TG) (**F**) and total cholesterol (TC) (**G**) were measured at week 4, 8 and 14. gWAT, gonadal white adipose tissue; iBAT, interscapular brown adipose tissue; sBAT, subscapular brown adipose tissue; sWAT, subcutaneous white adipose tissue. Data are shown as mean ± SEM. A: n=5 cages per group. B-G: n=15-16 mice per group. A-C, F and G: data were analyzed by two-way repeated-measures ANOVA and Bonferroni post hoc analysis. E: data were analyzed by unpaired two-tailed Student's t-test. *P<0.05.

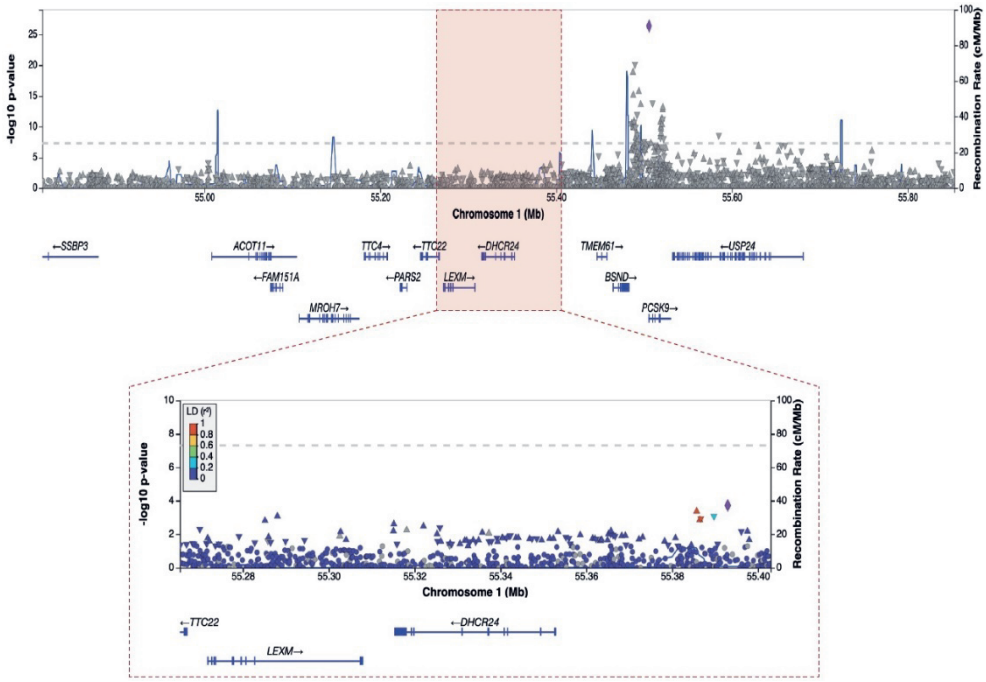

Fig. S2. Genetic association of *DHCR24* variants with coronary artery disease in humans. Locus zoom showing genetic associations of variants in the *DHCR24* locus (1p32.3, GRCh37); chr1:54,815,386-55,852,855 (Upper panel) and chr1:55,265,300-55,402,921 (lower panel) with coronary artery disease. The data comes from the genome-wide association study for coronary artery disease published by Aragam *et al*.[1] comprising 181,522 cases among 1,165,690 participants of predominantly European ancestry. Each symbol corresponds to individual genetic variants in the locus. The purple diamond corresponds to the variant with the lowest *P* value in the window. The color code represents the linkage disequilibrium (LD) in r^2, with the top associated variant (color scale in the top left-hand corner). The grey dotted line depicts the genome-wide significance *P* value threshold of 5×10^{-8}.

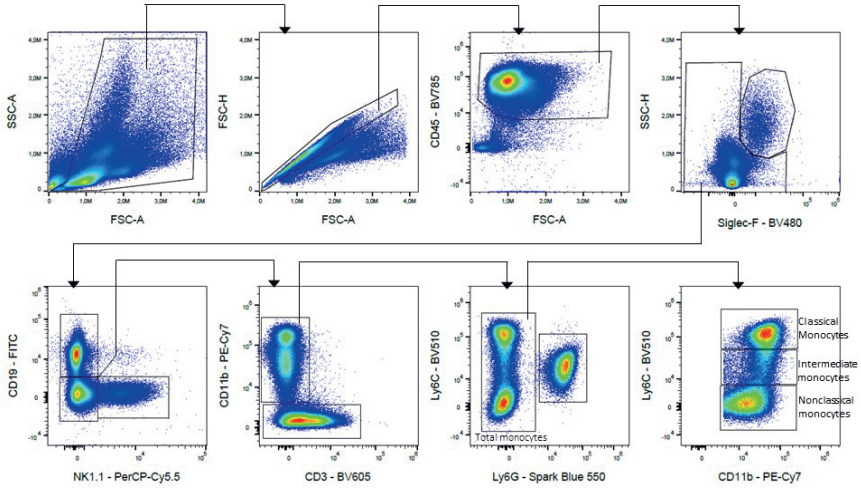

Fig. S3. Gating strategy for flow cytometry in blood leukocytes of APOE*3-Leiden.CETP mice, related to Figure 3C. APOE*3-Leiden.CETP (E3L.CETP) mice were fed a Western-type diet containing 16% fat and 0.15% cholesterol and received intraperitoneal injections with either SH42 (0.5 mg/mouse) or vehicle 3 times per week. After 15 weeks of treatment, blood samples were collected for flow cytometry. A representative gating strategy is presented.

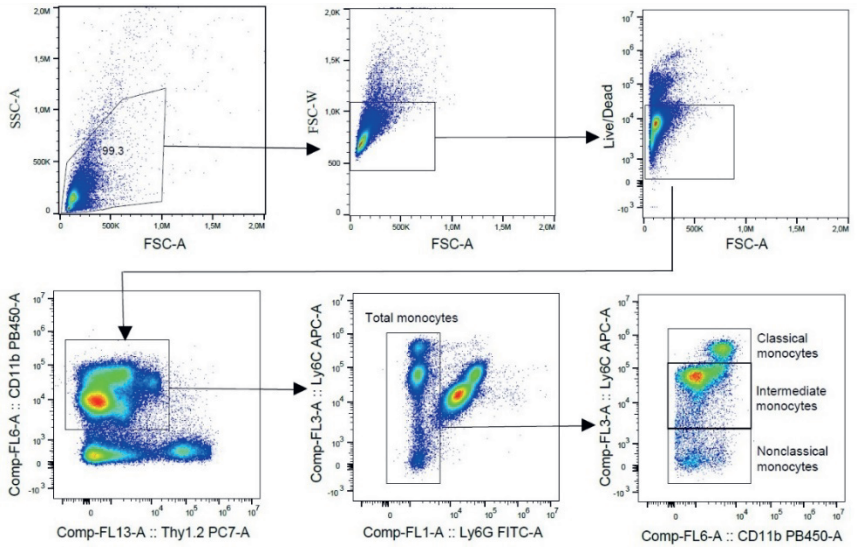

Fig. S4. Gating strategy for flow cytometry in blood leukocytes of LDL receptor knockout mice, related to Figure 5B. LDL receptor knockout (LDLr-KO) mice were fed a Western-type diet containing 16% fat and 0.25% cholesterol and received intraperitoneal injections with either SH42 (0.5 mg/mouse) or vehicle 3 times per week. After 12 weeks of treatment, blood samples were collected for flow cytometry. A representative gating strategy is presented.

Supplemental reference

1. Aragam K. G., Jiang T., Goel A.*, et al.* Discovery and systematic characterization of risk variants and genes for coronary artery disease in over a million participants. *Nat. Genet.* **54**, 1803–1815 (2022).